Microbiological Research 228 (2019) 126304

Contents lists available at ScienceDirect

Microbiological Research

journal homepage: www.elsevier.com/locate/micres

Pdh is involved in the cell division and Normal septation of *Streptococcus suis*

Yang Wang[a,b,*], Yuxin Wang[a,b], Jinpeng Li[a,b], Shenglong Gong[a,b], Liyun Sun[a,b], Daniel Grenier[c], Li Yi[d,**]

[a] College of Animal Science and Technology, Henan University of Science and Technology, Luoyang, China
[b] Key Laboratory of Molecular Pathogen and Immunology of Animal of Luoyang, Luoyang, China
[c] Groupe de Recherche en Écologie Buccale (GREB), Faculté de Médecine Dentaire, Université Laval, Quebec City, QC, Canada
[d] College of Life Science, Luoyang Normal University, Luoyang, China

ARTICLE INFO

Keywords:
S. suis
Pyruvate dehydrogenase
Cells chain
Z rings
Interaction
Cell division

ABSTRACT

Streptococcus suis (*S. suis*) is an important zoonotic pathogen that causes major economic losses in the pig industry worldwide. The *S. suis* cell division process is an integral part of its growth and reproduction, which is controlled by a complex regulatory network. Pyruvate dehydrogenase (PDH), which catalyzes the oxidative decarboxylation of pyruvate to form acetyl-CoA, while reducing NAD + to NADH, plays an important role in energy metabolism. Recently, we reported that *pdh* regulates virulence by reducing stress tolerance and biofilm formation in *S. suis* serotype 2. In this study, we found that deletion of the *pdh* gene in *S. suis* resulted in abnormal cell chains, plump morphology and abnormal localization of the Z rings, indicating that the knockout mutant is impaired in its ability to divide. In addition, the interaction between FtsZ and PDH in vitro was confirmed by ELISA, and qRT-PCR analysis revealed that the deletion of the *pdh* gene results in differential expression of the division-related genes *ftsZ, ftsK, ftsl, zapA, divIC, pbp1a, rodA, mreD,* and *sepF*. These results indicate that *pdh* is involved in the normal formation of Z rings and cell morphology during *S. suis* cell division.

1. Introduction

Streptococcus suis (*S. suis*) is a zoonotic pathogen worldwide that causes diseases such as sepsis, meningitis, pneumonia, endocarditis, and polyarthritis in humans and pigs. Bacterial cell division is a basic physiological process of bacterial growth and reproduction, and can be associated with potential target proteins for the development of new broad-spectrum antibacterial drugs (Foss et al., 2011; Hale and de Boer, 1997; Kenneth et al., 2011). In nature, bacteria exhibit a variety of growth patterns and morphology, suggesting that different species of bacteria may have different regulatory mechanisms for cell growth and division. The mechanisms of bacterial division have been more extensively studied in *Staphylococcus aureus*, *Streptococcus pneumoniae*, *Escherichia coli* and *Bacillus subtilis* (Foss et al., 2011).With regard to *S. suis*, the research on the mechanisms of cell division is still in its infancy. In general, ellipsoids perform splitting activities on the central axis of the cell along parallel planes perpendicular to the long axis. FtsZ plays a key role in cell division and can be polymerized into the Z ring to guide the formation and morphology of the membrane (Addinall and Lutkenhaus, 2010; Vishnyakov and Borchsenius, 2007). At the same time, studies have found that a variety of proteins can interact with FtsZ, which affects the protein assembly of FtsZ (Huo et al., 2016; Krupka et al., 2017; Ortiz et al., 2016; Skagia et al., 2017). The lack of knowledge regarding the process of cell division of *S. suis* limits the development of inhibitors of cell division.

The pyruvate dehydrogenase (PDH) gene is the first rate-limiting enzyme that catalyzes the pyruvate reaction, which is of great significance for the nutrient metabolism of organisms. PDH complex coordinates the conversion of pyruvate to acetyl-CoA under aerobic conditions or to lactic acid under anaerobic conditions (Jha et al., 2016). PDH is also considered as an important component of the bacterial skeleton (Dallo et al., 2010). At the same time, studies have shown that deletion of *pdh* can lead to impaired formation of *Streptococcus pneumoniae* capsules (Echlin et al., 2016). Previous studies have found that after the *pdh* gene is deleted by *S. suis*, the virulence of the strain in the mouse infection model is significantly reduced. Studies have shown that PDH is involved in the pathogenesis of *S. suis*, and reduction in virulence of strain may be related to the decreased ability to resist stress (Wang et al., 2019). However, whether PDH is associated with cell division and regulation of *ftsz* is still unknown.

In this study, the role of PDH in the growth and division of *S. suis* cells was first examined. After the deletion of *pdh*, the cells appear

* Corresponding author at: College of Animal Science and Technology, Henan University of Science and Technology, Luoyang, China.
** Corresponding author.
E-mail addresses: wangyocean@163.com (Y. Wang), lilili123168@163.com (Y. Li).

https://doi.org/10.1016/j.micres.2019.126304
Received 21 April 2019; Received in revised form 15 July 2019; Accepted 18 July 2019
Available online 02 August 2019
0944-5013/

plump in very long chains and the formation of Z rings was abnormal. Interaction assays between PDH and FtsZ showed that the two proteins interact together in vitro. Morever, real-time PCR experiments revealed that *pdh* gene deletion induces significant changes in the expression of division-related genes. Altogether, the results indicate that PDH plays an important role in maintaining normal morphology and division of *S. suis* cells.

2. Materials and methods

2.1. Bacterial strains and culture conditions

S. suis serotype 2 strain ZY05719 was isolated from an infected pig in Ziyang, China, in 2005 and confirmed to be a virulent strain (Liu et al., 2006). *S. suis* was cultivated in Todd-Hewitt broth (THB) (Difco Laboratories, Detroit, MI) or plated on THB solid plates containing 2% agar. Bacterial cultures were carried out under different conditions according to the experimental requirements. The *pdh* deletion mutant (Δ*pdh*) and complemented strain (CΔ*pdh*) were constructed in our laboratory (Wang et al., 2019). *Escherichia coli* (*E. coli*) strains DH5α andBL21 (DE3) were cultured in Luria-Bertani (LB) medium or on LB solid plates containing 2% agar. When appropriate, spectinomycin at a concentration of 100 μg / mL or ampicillin at a concentration of 50 μg / mL was added. Related strains are listed in Table 1.

2.2. Identification of Δpdh strain

The Δ*pdh* strain was added to THB liquid medium and cultured for 8 h at 37 °C. Then, PCR was double-identified with the outer primers *pdh*-X and *pdh*-Y and the internal primers *pdh*-ORF-1 and *pdh*-ORF-2, while the wild-type strain was used as the control group. Related primers are listed in Table 2.

2.3. Microscopic observations

Cells of *S. suis* (WT, Δ*pdh*, CΔ*pdh*) were collected at mid-log phase and washed twice with phosphate buffer saline (PBS). Twenty μL of each sample was then heat-fixed on a glass slide. Gram stain kit (Jiancheng, China) was used according to the manufacturer's instructions. The stained samples were observed using an optical microscope 40× oil mirror (Primo Star; Zeiss, Gödingen, Germany).

Scanning electron microscopy (SEM) was performed as previously described with small modifications (Shi et al., 2014). All three strains (WT, Δ*pdh*, CΔ*pdh*) were grown in THB liquid medium. Cells were spotted onto polylysine coverslips and washed with PBS. The cells were fixed at 48 °C for 1 h with 2% glutaraldehyde. The subsequent dehydration step was performed in ethanol and the samples were air-dried. Finally, the samples were placed in an evaporator and coated with gold/palladium. Observation was carried out at 5 kV with a scanning electron microscope (Model S800; Hitachi, Tokyo, Japan). One hundred bacterial cells of each strain were randomly selected from SEM micrographs, and cell size was measured using Image J. The data were then statistically analyzed using GraphPad Prism 6.

Transmission electron microscopt (TEM) was performed as previously described with minor modifications (Gao et al., 2016). Cells from cultures of *S. suis* (WT, Δ*pdh*, CΔ*pdh*) were harvested by centrifugation, and then fixed overnight with 2.5% glutaraldehyde (1 mL). The cells were treated with 2% osmium tetroxide in the dark for 2 h. Subsequent dehydration steps were performed in ethanol at50% for 15 min, 70% for 15 min, 95% for 15 min, and 100% for 20 min. The dehydrated cells were embedded in an epoxy resin, and cell morphology were observed using H-7650 TEM (Hitachi, Tokyo, Japan).

Table 2
Primers used in this study.

Primers	Sequence (5′-3′)	Source of references
pdh-X	CCAATGGGATAAGGGTA	This work
pdh-Y	TGTTTCATTGACGAGTAAA (2685 bp)	
pdh-ORF-1	CATGATGGCTGAGCTTGC	This work
pdh-ORF-2	TAAGCGTGTTCTTTCGGG (681 bp)	
pdh-F	CGCGAATTCATGCAACAAATCCGTGAT (*EcoR*I)	This work
pdh-R	CCCTCGAGGCTAGTCTACAAACACATC (*Xho*I) (924bp)	
ftsZ-F	CGCGGATCCATGGCATTTTCATTTGAAGCA (*BamHI*)	This work
ftsZ-R	CCGGAATTCTTAGCGATTACGGAAGAATGG (*EcoR*I) (1230bp)	

2.4. Analysis of bacterial sedimentation

Bacterial sedimentation was analyzed as described previously with minor modifications (Hesketh et al., 2002). The WT, Δ*pdh* and CΔ*pdhS. suis* strains were inoculated in THB medium (1% v/v inoculum), respectively, and cultivated overnight at 37 °C. Prior to initiate the experiment, the bacterial suspensions were vortexed for 15 s, and allowed to stand at room temperature. By measuring the optical density at 600 nm ($OD_{600\ nm}$) at every 30 min intervals in the upper half of the tubes, the degree of aggregation was determined. The impact of PDH in bacterial sedimentation was examined by measuring the sedimentation rate of WT, Δ*pdh* and CΔ*pdh* strains.

2.5. Overexpression and purification of PDH and FtsZ

DNA manipulations were performed as previously described (Marilena et al., 2014; Shi et al., 2014), First, the chromosomal DNA of *S. suis* ZY05719 was used as a template, and then the target gene was obtained by PCR amplification using the *pdh*-F / *pdh*-R or *ftsZ*-F/*ftsZ*-R primers listed in Table 2. Next, the recombinant plasmid was extracted, digested and inserted into the His-tagged pET32a expression vector to obtain a recombinant plasmid pET32a-*pdh* or pET32a-*ftsZ*, which was transferred to competent cell BL21 (DE3). To obtain the purified protein, 0.5 mM isopropyl-b-D-thiogalactopyranoside (IPTG) (Sigma, USA) was added to the bacterial culture and expression was induced at 37 °C for 8 h. The protein was further purified by gel filtration chromatography using a Superdex-200 10/300 G L column (GE Healthcare, Sweden) and stored at −80 °C. His-tagged PDH was used to immunize mice to produce polyclonal antibodies.

Table 1
Bacterial strains used in this study.

Strains/plasmids	Relevant characteristics	Source of references
Strains		
S. suis ZY05719	One of the most toxic strains; isolated from dead pig	Collected in our laboratory
ZY05719 Δ*pdh*	ZY05719 has no PDH functional strain	Collected in our laboratory
ZY05719 CΔ*pdh*	Complemented strain of ZY05719 Δ*pdh*	Collected in our laboratory
E. coli DH5α	DH5a is a strain commonly used for plasmid cloning	Collected in our laboratory
E. coli BL21 (DE3)	Host for expressing the recombinant protein	Collected in our laboratory

2.6. Ethics statement

All animal experiments in this study were approved by the Experimental Animal Monitoring Committee of Henan University of Science and Technology and carried out accordingly.

2.7. Interaction assay for PDH and FtsZ

Protein-protein interaction assay was performed according to the procedure of Shi et al. with small modifications (Shi et al., 2014). Briefly, 500 μg of purified FtsZ or bovine serum albumin (BSA) (Solarbio, USA) was added to a buffer containing 14 mM Na_2CO_3 and 36 mM $NaHCO_3$, and then coated onto an enzyme-linked immunosorbent assay plate at 4 °C (overnight). The plate was taken and washed three times with PBS containing 0.5% Tween-20 (PBST) to remove unbound protein. Non-specific binding sites were blocked by incubation with PBS buffer containing 10% goat serum for 2 h at 37 °C. The purified PDH protein was then diluted to different concentrations using PBS, and different concentrations of PDH protein were added to the wells and incubated for 2 h at 37 °C. The assay plate was then washed three times with PBST. Finally, the interaction between PDH and FtsZ was detected using a mouse anti-PDH antibody as primary antibody and horseradish peroxidase-labeled goat anti-mouse antibodies as secondary antibody (BioRad, Hercules, CA). BSA-coated wells were used as negative controls. The assays were performed in triplicate.

2.8. Quantitative real-time PCR (qRT-PCR) analysis

qRT-PCR analysis was performed as previously described with minor modifications (Wang et al., 2011). *S. suis* (WT and Δ*pdh*) were inoculated into THB and grown overnight at 37 °C. Afterwards, the cells were transferred to fresh THB medium (1% v/v inoculum) and bacterial cells were collected in the logarithmic growth phase. RNA was isolated by using TRizol reagent (TaKaRa, Dalian, China). DNA was removed using DNase I (TaKaRa, Dalian, China). The cDNA was synthesized according to the instructions of the Prime ScriptTM RT Kit (TaKaRa, Dalian, China).The WT strain was used as a control group, and the mRNA expression level was detected by qRT-PCR (*16 s rRNA* as a housekeeping gene). The fluorescent quantitative PCR primers for the 9 genes and the internal reference gene *16 s rRNA* are shown in Table 3 (Orietta et al., 2013). The experiment used the SYBR Green PCR method, and the kit used was SYBR Premix Ex TaqTM kit (TaKaRa, Dalian, China). qRT-PCR experiments were performed using an ABI 7300 RT-PCR system (Applied Biosystems). In order to confirm the unity and accuracy of the PCR product, we performed dissociation analysis on the detected data. The mRNA level analysis method is a comparison cycle threshold method ($2^{-\triangle\triangle CT}$ method) (Livak and Schmittgen, 2001). Assays were performed in triplicate. All data are given in terms of relative quantities of mRNA expressed as the means plus.

Table 3
9 kinds of genes and *16 sRNA* fluorescent qRT-PCR primers.

Name	Sequence (5′-3′)	Target gene
16 s rRNA-S	GTTGCGAACGGGTGAGTAA	*16 s rRNA*
16 s rRNA-A	TCTCAGGTCGGCTATGTATCG	
FtsZ-S	TGAGGAAAGCGAAGAAGCAT	*ftsZ*
FtsZ-A	AAACCAAACGGACGAGTCAC	
FtsK-S	AAAGATAAGTTGGTGGAGAC	*ftsK*
FtsK-A	CTACCAGTGCCAAAGCCC	
FtsL-S	AGTCTTCTCAGTTCAGCAAA	*ftsl*
FtsL-A	GAGATATTCTTACCTAAGGTC	
ZapA-S	ATGGAAGAGATTGAGCGTAT	*zapA*
ZapA-A	GAGATATTCTTACCTAAGGTC	
DivIC-S	GCCTGCCTATAATCTTGTTG	*divIC*
DivIC-A	TTGCTCGGTATTCCTCATTT	
PBP1a-S	GCTGACTTATTTCTCGACAT	*pbp1a*
PBP1a-A	GTCTTCATACCGTAATTACC	
RodA-S	AGTCCAGACTTAGTAGCATC	*rodA*
RodA-A	ATCACCCTTGACAACATAATG	
MreD-S	ATTGGTCGGTCGGATTATTT	*mreD*
MreD-A	GTTGTAGTAGCAATACCAATC	
SepF-S	TGAAAGGCAGCAAGAATTGA	*sepF*
SepF-A	TACTGAACGAGCACCATCCA	

2.9. Statistical analysis of test data

The GraphPad Prism version 6 software was used to perform statistical analyses for all data. All data points for the experiments, performed in triplicate, were analyzed using the single factor analysis of variance (One - Way ANOVA), where $P < 0.05$ was considered to be statistically significant.

3. Results

3.1. Identification of S.suis Δpdh strain

To investigate the PDH function in *S. suis*, we used the correct Δ*pdh* strain (Supplementary material, Fig. S1) and CΔ*pdh* strain (data not shown) in this study.

3.2. Deletion of the pdh gene leads to abnormal cell division

In order to further analyze the growth phenotype of the Δ*pdh* strain, we performed a Gram staining and sedimentation test for the three strains (WT, Δ*pdh*, CΔ*pdh*). The results showed that the chain length of the Δ*pdh* strain was longer than that of the WT strain (Fig. 1A and B). At the same time, the Δ*pdh* strain exhibited a higher sedimentation rate, and the difference was extremely significant ($P < 0.01$) (Fig. 1D). The sedimentation states of WT, Δ*pdh*, CΔ*pdh* strains at 300 min are shown in Fig. 1E. The results showed that there was a significant difference in the chain length and growth state of *S. suis* after deletion of the *pdh* gene compared with WT.

3.3. Deletion of the pdh gene causes the S. suis Z rings delocalization

To further clarify the mechanism by which the *pdh* gene affects *S. suis* cell division, SEM and TEM of the WT strain and Δ*pdh* strain were used to compare the cell morphology (Fig. 2). A marked difference was that the Δ*pdh* strain appeared as long bacterial chains with unsplit cross-wall joined cells. More specifically, the long chains of bacteria observed often involved more than 20 cells (Fig. 2B1). When observing the cell morphology of the Δ*pdh* strain, we also found that compared with the WT strain, the cell morphology does not show a normal ellipsoid but rather a globular shape (Fig. 2 B1). Comparing the morphology of Δ*pdh* strain and WT strain by SEM and TEM revealed that WT strain had a typical egg-like shape and division pattern (Fig. 2A). In contrast, the Δ*pdh* strain showed abnormal ultrastructure (crimp aspect) or Z rings formation was not localized at the equator (Fig. 2B).

Cell length and width were quantified to more accurately determine the morphological phenotype of the Δ*pdh* strain (Fig. 3 and Fig. 4). Individual cells were randomly selected from membrane-stained cells for longitudinal length measurements. The statistical results of the cell length distribution of the WT strain, the Δ*pdh* strain and the CΔ*pdh* strain are shown in Fig. 3. Among them, the cell length of the WT strain and the CΔ*pdh* strain were mainly concentrated between 1.0 and 1.8 μm, and the cell length of the Δ*pdh* strain was concentrated between 1.0 and 1.3 μm (Fig. 3). At the same time, we calculated the average cell length of the Δ*pdh* strain along the long axis of the cell to be 1.28 μm, compared to 1.43 μm in WT cells and 1.40 μm in CΔ*pdh* cells (Fig. 4A). And the cell length of Δ*pdh* strain was shorter compared with WT and CΔ*pdh* strains ($P < 0.05$). The average width of Δ*pdh* cells was calculated to be 0.8467 μm along the horizontal axis of the cells, the

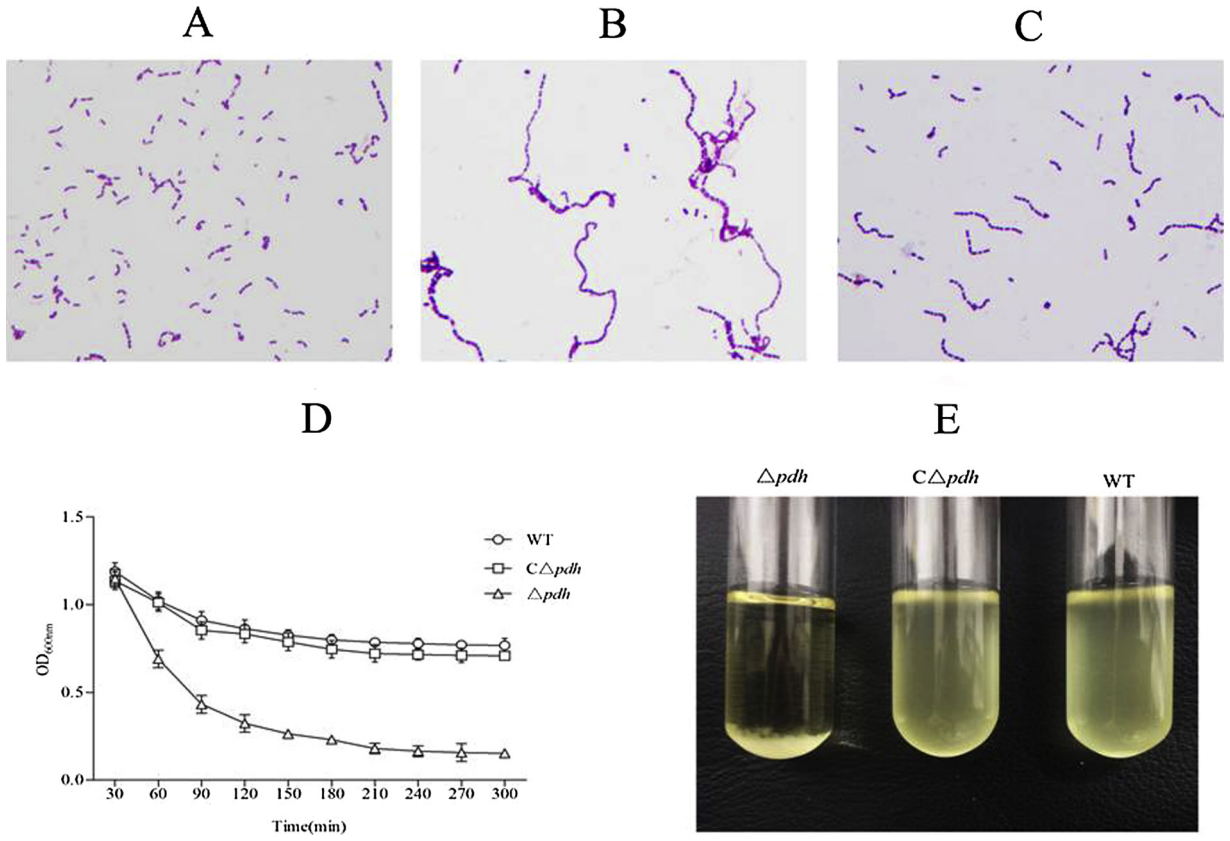

Fig. 1. Bacterial morphology and bacterial sedimentation of the WT, Δ*pdh* and CΔ*pdh* strains.
A: WT strain, B: Δ*pdh* strain, C: C△*pdh* strain. All images were magnified 1000 times. D: Sedimentation rate curve of the three strains determined by monitoring the OD_{600nm} value of the upper portion of the tube at different time points. E: Visual observation of bacterial sedimentation after 300 min of incubation.

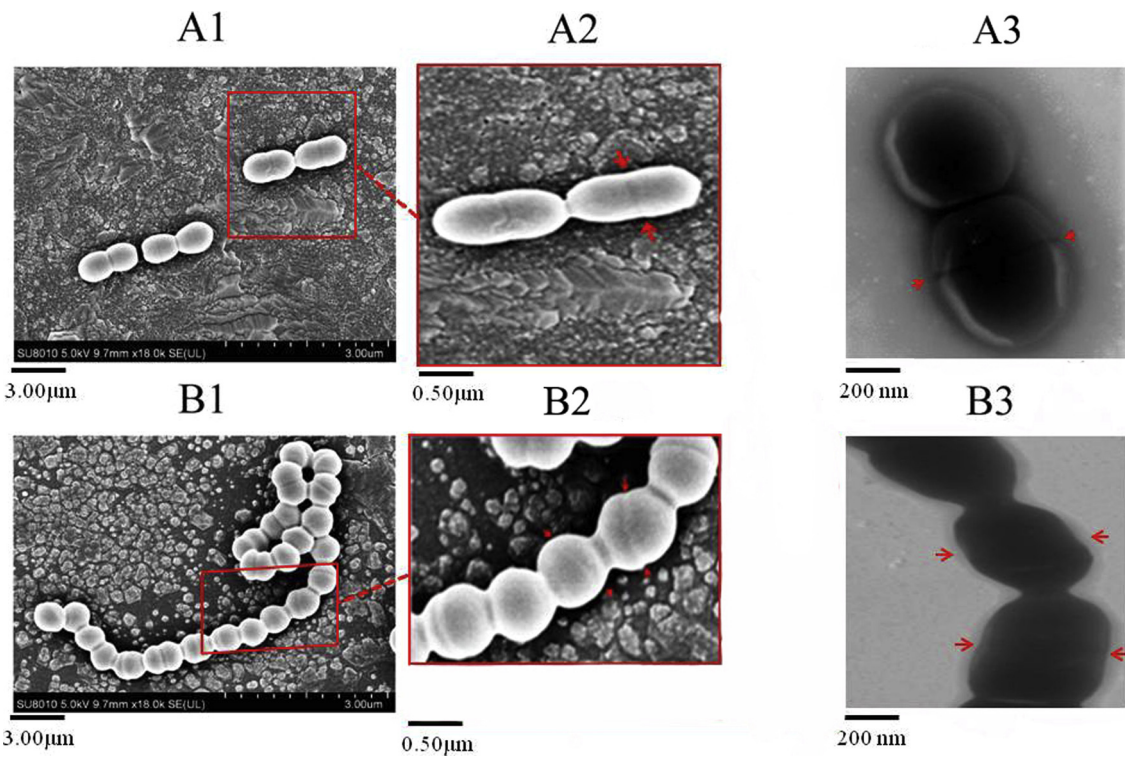

Fig. 2. Micrograph of *S. suis* WT and Δ*pdh*.
1. A1 (Scale bar, 3 μm) and A2 (Scale bar, 0.5 μm) are SEM photographs of WT strain, and A3 (Scale bar, 200 nm) is a TEM photograph of WT strain. 2. B1 (Scale bar, 3 μm) and B2 (Scale bar, 0.5 μm) are SEM photographs of the Δ*pdh* strain, and B3 (Scale bar, 1 μm) is a TEM photograph of the Δ*pdh* strain. Note: The red arrow indicates the position and orientation of the Z rings.

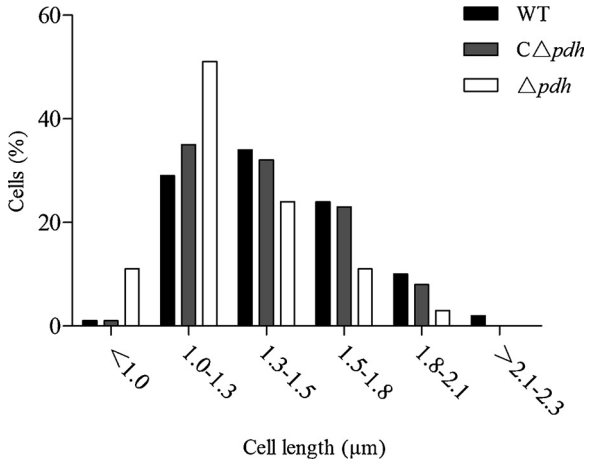

Fig. 3. Cell length distribution of *S. suis* strains as determined by SEM.
Histograms of WT (n = 100, black), Δ*pdh* (n = 100, white) and CΔ*pdh* (n = 100, gray) cells counted following growth in THB medium. To determine cell length, we measured the longitudinal length of individual membrane stained cells. Δ*pdh* cells were significantly shorter than WT cells ($P < 0.01$).

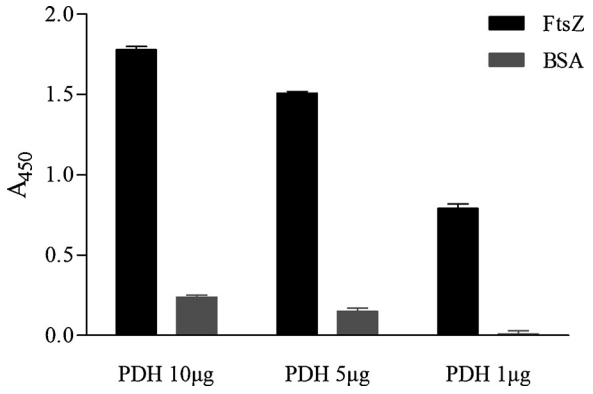

Fig. 5. Solid phase binding assay of FtsZ and PDH.
The wells of the microtiter plates were coated with FtsZ or BSA and incubated with various concentrations of PDH protein as indicated.

average width of WT cells was 0.79 μm, and 0.7967 μm in CΔ*pdh* cells ($P < 0.05$) (Fig. 4B). These data suggest that *pdh* has a complex regulatory function in *S. suis* cell division.

3.4. PDH interacts with FtsZ in vitro

The FtsZ protein is an important cell division initiation factor. The formation of Z rings observed by TEM and SEM involves an interaction between PDH and FtsZ. To assess the physical interaction between PDH and FtsZ proteins of *S. suis* in vitro, we first constructed a prokaryotic expression vector to obtain purified PDH and FtsZ (Supplementary material, Fig. S2). FtsZ- or BSA-coated ELISA plates were incubated with 10 μg, 5 μg, and 1 μg of purified PDH and bound PDH was determined using a soecific antibody. The washed PDH was immunolabeled and quantified by ELISA. The results showed that PDH is able to bind to FtsZ but does not substantially bind to BSA (Fig. 5).

3.5. pdh regulates the expression of genes involved in cell division

It has been reported that in *Streptococcus pneumoniae*, a total of 33 proteins are involved in the process of bacterial cell division (Orietta et al., 2013). In order to determine whether there are changes in the transcriptional levels of other cell division-related genes in Δ*pdh*, we performed qRT-PCR on 33 genes in WT strain and △*pdh* strain that have been explicitly involved in *S. pneumoniae* cell division. The gene expression levels of 9 genes (*ftsZ*, *ftsK*, *ftsl*, *zapA*, *divIC*, *pbp1a*, *rodA*, *mreD* and *sepF*) were significantly different ($P < 0.05$) or highly significantly ($P < 0.01$) (Table 4).

4. Discussion

The normal cellular morphology of *S. suis* is ellipsoidal, and the cleavage site is located in the middle of the bacterium, which is continuously perpendicular to the long axis of the bacterium. Studying the cell division of bacteria does not only provide information about this basic biological process, but also helps to explore potential drug targets and lay the foundation for the development of new broad-spectrum antibacterials. Here, the data suggest that PDH plays an important role in *S. suis* cell division.

PDH is a multi-enzyme complex widely distributed in microorganisms, mammals, and higher plants. Pyruvate produced by the bacterial glycolytic pathway produces acetyl CoA through the PDH, enters the tricarboxylic acid cycle, and produces energy through oxidative phosphorylation (Bonnet et al., 2007). However, when the PDH function is defective, the cells often use other pathways, called PDH bypass, for energy metabolism (Lapointe et al., 2002; Zeeman et al., 1998). This study found that *pdh* deletion did not affect the viability of the cells of *S. suis*. It is speculated that cells may undergo energy compensation through PDH bypass. The role of PDH in cells is mainly involved in the metabolism of pyruvate, catalyzing the oxidative decarboxylation of pyruvate to form Acetyl-CoA, while reducing NAD + to NADH. Studies have reported that metabolic proteins such as Ga5DH, ManA and UgtP affect the cell structure and cell division of *S. suis* and *B. subtilis* (Elbaz

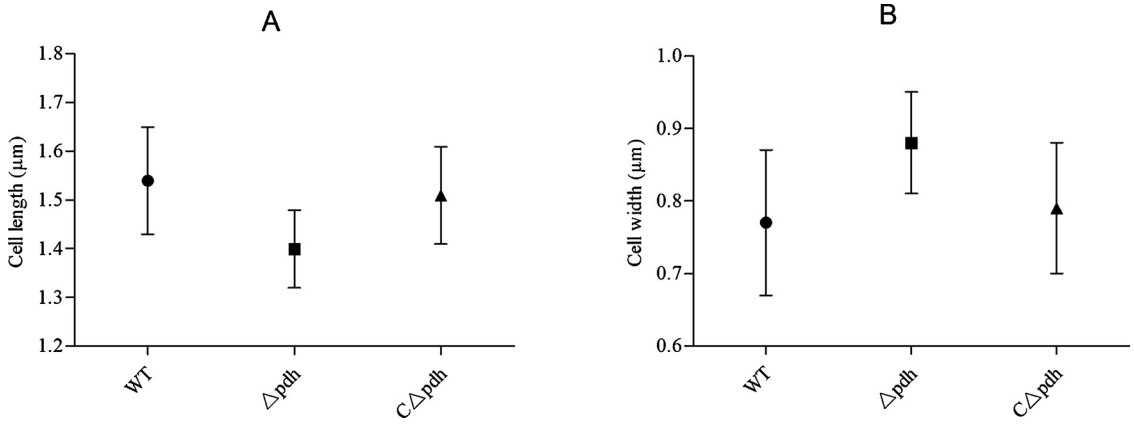

Fig. 4. Mean of cell size for WT, Δ*pdh* and CΔ*pdh* *S. suis* strains.
The cell length of the Δ*pdh* strain was significantly different from that of the WT strain ($P < 0.01$; two-tailed t-test).

Table 4
Differences in transcriptional levels of cell division genes (△*pdh* / WT).

Gene	Locus	Function	Fold difference in mRNA level (± SD)
ftsZ	ZY05719_RS02380	Cytoskeletal structure, forms a cytoplasmic ring structure at midcell.	0.067 (± 0.008)
ftsK	ZY05719_06375	Recruitment of proteins and DNA transport.	0.011(± 0.001)
ftsl	ZY05719_RS08235	Unknown; role in septal PG synthesis?	0.013(± 0.002)
zapA	ZY05719_RS01230	Stabilization of FtsZ polymers.	0.119(± 0.007)
divIC	ZY05719_RS00050	Interactions with peptidoglycan synthases; septal PG synthesis.	0.021(± 0.004)
pbp1a	ZY05719_RS02005	PG glycosyltransferase/transpeptidase; peripheral and septal PG synthesis.	13.889(± 2.883)
rodA	ZY05719_RS07140	Lipid II flippase; peripheral PG synthesis.	0.837 (± 0.023)
mreD	ZY05719_RS00190	MreB-associated and inner membrane-associated protein; role in peripheral PG synthesis.	0.323 (± 0.034)
sepF	ZY05719_RS02390	Z-ring positive regulator.	0.025(± 0.003)

and Ben-Yehuda, 2010; Shi et al., 2014; Weart et al., 2007). These effects mainly result from the accumulation of high concentrations of sugar directly interacting with related enzymes, thereby inhibiting FtsZ assembly and delaying the maturation of the Z ring. PDH is likely to play a similar role, although it needs to be confirmed.

The results of Gram staining showed that the cell chains of the Δ*pdh* strain were longer than that of the WT strain and the difference was highly significant ($P < 0.01$). Moreover, cells of the Δ*pdh* strain showed a higher sedimentation rate. This phenotype appears to be specific because there is no significant difference between the CΔ*pdh* strain and the WT strain. By measuring the sedimentation rate of the WT, Δ*pdh* and CΔ*pdh* strains, it was further confirmed that abnormal bacterial cell division may enhance aggregate formation and the observed sedimentation. These results are in agreement with those of Gallotta et al. regarding group A *Streptococcus* (Marilena et al., 2014).

Abnormal bacterial cell division is often reflected in cell morphology and changes in the chain length of bacteria. Studies have showed that the deletion of the *S. suis* gluconate metabolic enzyme gene *ga5dh* results in increased length of bacterial cells and a non-contracted membrane (Shi et al., 2014). *S. suis* response regulator CovR globally regulates gene expression and negatively regulates the virulence of *S. suis*; the capsule of a deficient-mutant becomes thinner and bacteria produce longer chains than the parent strain (Xiuzhen et al., 2009). XerC and XerD belong to the tyrosine recombinase family and mediate site-specific recombination of circular chromosomes, which are present in *streptococcus* and lactic acid bacteria, while its homologue XerS is found in *S. suis*. The XerS deletion mutant of *S. suis* grows slowly, presents morphological changes and produces long chains (Maxime et al., 2011). Fleurie et al. brought evidence that the dislocation of pneumococcal StkP can eliminate its function and affect cell division (Aurore et al., 2012). In this study, the deletion of the *S. suis pdh* gene caused bacterial cells to form very long chains compared to the WT strain. This change in chain length was highly significant ($P < 0.01$). At the same time, the morphology of the cells also changed. The Δ*pdh* cell showed a shortened cell length and a non-contracted membrane. These findings fully demonstrate that multiple proteins are involved in the regulation of normal division of bacterial cells, and the PDH gene is likely to be one of them.

The *S. suis* splitting assembly pattern is similar to that of *Streptococcus pneumoniae*. The skeletal protein FtsZ is the protein that first enters the cleavage site and self-polymerizes to form the Z-ring, recruiting a variety of downstream proteins as scaffolds and triggering the assembly of large protein complexes. The initiation of cell membrane synthesis, first introduced into the division, is the cell division initiation proteins FtsZ and FtsA, followed by the synthesis of the marker proteins DivlB (FtsQ), DivlC (FtsB), FtsL, FtsW, PBPla, PBP2X and the cell division protein DivlVA. After the Z ring is formed, it enters the cleavage site (Orietta et al., 2013). Many studies have shown that a variety of proteins can interact with FtsZ, affecting the abnormal formation of Z-rings in bacterial cells, leading to abnormal cell division. Pneumococcal PBP2b28 mutant cells showed a rod shape (Orio et al., 2011). TEM showed that the rod cells presents multiple membranes and suggested that PBP2b28, which has a direct interaction with FtsZ, can lead to mislocalization of FtsZ and abnormal cell morphology. Studies have shown that deletion of PDH E1α causes *Bacillus subtilis* cells to exhibit Z-ring formation defects (Monahan et al., 2014). This is very consistent with this study. However, there is no research to determine whether PDH E1α binds FtsZ directly or via an interaction partner to coordinate regulation activities. In this study, we first confirmed that PDH can interact directly with FtsZ. By observing the cell morphology of △*pdh* strain under SEM and TEM, it was confirmed that the deletion of PDH resulted in abnormal localization of Z rings in the cells. But does PDH have an effect on FtsZ protein assembly? Or does it have a direct or indirect effect on subsequent cell division? We also examined the effect of *pdh* on the expression of 33 genes involved in *S. suis* division, and found that the expression levels of 9 genes changed significantly. The expression of *ftsZ* gene was significantly down-regulated, which directly affected the production of FtsZ protein. In addition, the expression level of the PBP1a, which promotes the synthesis of the septal cell wall, was significantly up-regulated. This may impede the longitudinal extension of cell division and increase the rate of cell septum division (André et al., 2010; Dennis et al., 2010; Steele et al., 2011). This is likely one of the reasons why the Δ*pdh* cells are plump and long chains.

5. Conclusions

In conclusion, this study demonstrated for the first time that the *pdh* gene plays an important role in *S. suis* cell division. The deletion of the *pdh* gene does not substantially affect the growth rate of *S. suis*, but causes the cells to be arranged as longer cell chains, and to present plump cell morphology and Z rings abnormally located. A better knowledge of PDH function may reveal other components of the mechanism of cell division of *S. suis* and provide new potential targets for drug treatment interventions for *S. suis* disease.

Author contributions

Conceived and designed the experiments: YW and LY. Performed the experiments: YXW and JPL. Analyzed the data: YW, YXW and SLG. Contributed reagents/materials/analysis tools: LYS and JPL. Wrote the paper: YW and YXW. DG critically read and corrected the manuscript. All authors read and approved the final manuscript.

Declaration of Competing Interest

The authors have not declared any conflict of interest.

Acknowledgements

This study was funded by the National Natural Science Foundation of China (31772761), the Natural Science Foundation of Henan Province (182300410047).

Appendix A. Supplementary data

Supplementary material related to this article can be found, in the online version, at doi:https://doi.org/10.1016/j.micres.2019.126304.

References

Addinall, S.G., Lutkenhaus, J., 2010. FtsZ-spirals and -arcs determine the shape of the invaginating septa in some mutants of Escherichia coli. Mol. Microbiol. 22, 231–237. https://doi.org/10.1046/j.1365-2958.1996.00100.x.

André, Z., Thierry, V., Pinho, M.G., 2010. The different shapes of cocci. FEMS Microbiol. Rev. 32, 345–360. https://doi.org/10.1111/j.1574-6976.2007.00098.x.

Aurore, F., Caroline, C., Sébastien, G., Céline, F., Frédéric, G., Isabelle, Z.C., Anne-Marie, D.G., Christophe, G., 2012. Mutational dissection of the S/T-kinase StkP reveals crucial roles in cell division of Streptococcus pneumoniae. Mol. Microbiol. 83, 746–758. https://doi.org/10.1111/j.1365-2958.2011.07962.x.

Bonnet, S., Archer, S.L., Allalunis-Turner, J., Haromy, A., Beaulieu, C., Thompson, R., Lee, C.T., Lopaschuk, G.D., Puttagunta, L., Bonnet, S., 2007. A Mitochondria-K channel Axis Is suppressed in Cancer and its normalization promotes apoptosis and inhibits Cancer growth. Cancer Cell 11, 37–51. https://doi.org/10.1016/j.ccr.2006.10.020.

Dallo, S.F., Kannan, T.R., Blaylock, M.W., Baseman, J.B., 2010. Elongation factor Tu and E1 beta subunit of pyruvate dehydrogenase complex act as fibronectin binding proteins in Mycoplasma pneumoniae. Mol. Microbiol. 46, 1041–1051. https://doi.org/10.1046/j.1365-2958.2002.03207.x.

Dennis, C., Robyn, E., Hamoen, L.W., Daniel, R.A., Jeff, E., Edwards, D.H., 2010. Control of the cell elongation-division cycle by shuttling of PBP1 protein in Bacillus subtilis. Mol. Microbiol. 68, 1029–1046. https://doi.org/10.1111/j.1365-2958.2008.06210.x.

Echlin, H., Frank, M.W., Iverson, A., Chang, T.C., Johnson, M.D., Rock, C.O., Rosch, J.W., 2016. Pyruvate oxidase as a critical link between metabolism and capsule biosynthesis in Streptococcus pneumoniae. PLoS Pathog. 12, 1–28. https://doi.org/10.1111/j.1365-2958.2008.06210.x.

Elbaz, M., Ben-Yehuda, S., 2010. The metabolic enzyme ManA reveals a link between cell wall integrity and chromosome morphology. PLoS Genet. 6, e1001119. https://doi.org/10.1371/journal.pgen.1001119.

Foss, M.H., Eun, Y.J., Weibel, D.B., 2011. Chemical-biological studies of subcellular organization in bacteria. Biochemistry 50, 7719–7734. https://doi.org/10.1021/bi200940d.

Gao, T., Tan, M., Liu, W., Zhang, C., Zhang, T., Zheng, L., Zhu, J., Li, L., Zhou, R., 2016. GidA, a tRNA Modification Enzyme, contributes to the Growth, and Virulence of *Streptococcus suis* serotype 2. Front. Cell. Infect. Microbiol. 6, 1–11. https://doi.org/10.3389/fcimb.2016.00044.

Hale, C.A., de Boer, P.A., 1997. Direct binding of FtsZ to ZipA, an essential component of the septal ring structure that mediates cell division in E. Coli. Cell 88, 175. https://doi.org/10.1016/S0092-8674(00)81838-3.

Hesketh, P.J., Nauman, C.J., Hesketh, A.M., LaPointe, J., Fogarty, K., Oo, T.H., Lau, D.H., Edelman, M.J., Gandara, D.R., 2002. Unfavorable therapeutic index of cisplatin/gemcitabine/vinorelbine in advanced non-small-cell lung cancer. Clin. Lung Cancer 4, 47–51. https://doi.org/10.3816/CLC.2002.n.015.

Huo, Y., Lu, Q., Zheng, X., Ma, Y., Lu, F., 2016. E75, R78 and D82 of *Escherichia coli* FtsZ are key residues for FtsZ cellular self-assembly and FtsZ-MreB interaction. Acta Microbiol. Sin. 56, 264–274.

Jha, M.K., Lee, I.K., Suk, K., 2016. Metabolic reprogramming by the pyruvate dehydrogenase kinase-lactic acid axis: linking metabolism and diverse neuropathophysiologies. Neurosci. Biobehav. Rev. 68, 1–19. https://doi.org/10.1016/j.neubiorev.2016.05.006.

Kenneth, B., Peter, P., Dias, M.J., Jeanette, H., David, D., 2011. Maf acts downstream of ComGA to arrest cell division in competent cells of B. Subtilis. Mol. Microbiol. 81, 23–39. https://doi.org/10.1111/j.1365-2958.2011.07695.x.

Krupka, M., Rowlett, V.W., Morado, D., Vitrac, H., Schoenemann, K., Liu, J., Margolin, W., 2017. *Escherichia coli* FtsA forms lipid-bound minirings that antagonize lateral interactions between FtsZ protofilaments. Nat. Commun. 8, 15957. https://doi.org/10.1038/ncomms15957.

Lapointe, J.Y., Gagnon, M.P., Gagnon, D.G., Bissonnette, P., 2002. Controversy regarding the secondary active water transport hypothesis. Biochem. Cell Biol. 80, 525–533. https://doi.org/10.1139/o02-150.

Liu, J., Shi, Q., Sun, Y., Zhang, D., Yin, T.Y., Guo, X.J., Gao, H.W., Chang-Chun, T.U., Feng, S.Z., 2006. Identification and characterization of *Streptococcus suis* serotype 2 isolated from diseased pigs in Ziyang area of Sichuan province. Chin. J. Zoonoses 22, 1095–1099. https://doi.org/10.1007/s00034-004-1208-7.

Livak, K.J., Schmittgen, T.D., 2001. Analysis of relative gene expression data using real-time quantitative PCR and the 2 $-\Delta\Delta$ C t method. Methods-A Companion Methods Enzymol. 25, 402–408.

Marilena, G., Giovanni, G., Giampiero, P., Marirosa, M., Alfredo, P., Giovanna, T., Emiliano, C., Vincenzo, N.D., Anna Rita, T., Simonetta, R., 2014. SpyAD, a moonlighting protein of group A *Streptococcus* contributing to bacterial division and host cell adhesion. Infect. Immun. 82, 2890. https://doi.org/10.1128/IAI.00064-14.

Maxime, L., Fuli, J., George, S., 2011. Characterization of the *Streptococcus suis* XerS recombinase and its unconventional cleavage of the difSL site. FEMS Microbiol. Lett. 324, 135–141. https://doi.org/10.1111/j.1574-6968.2011.02398.x.

Monahan, L.G., Hajduk, I.V., Blaber, S.P., Charles, I.G., Harry, E.J., 2014. Coordinating bacterial cell division with nutrient availability: a role for glycolysis. Mbio. 5https://doi.org/10.1128/mBio.00935-14. 00935-00914.

Orietta, M., Linda, N., Waldemar, V., 2013. From models to pathogens: how much have we learned about *Streptococcus pneumoniae* cell division? Environ. Microbiol. 15, 3133–3157. https://doi.org/10.1111/1462-2920.12189.

Orio, A.G.A., Piñas, G.E., Cortes, P.R., Cian, M.B., Echenique, J., 2011. Compensatory evolution of *pbp* mutations restores the fitness cost imposed by β-lactam resistance in *Streptococcus pneumoniae*. PLoS Pathog. 7, e1002000. https://doi.org/10.1371/journal.ppat.1002000.

Ortiz, C., Kureisaite-Ciziene, D., Schmitz, F., Mclaughlin, S.H., Vicente, M., Löwe, J., 2016. Crystal structure of the Z-ring associated cell division protein ZapC from Escherichia coli. FEBS Lett. 589, 3822–3828. https://doi.org/10.1016/j.febslet.2015.11.030.

Shi, Z., Xuan, C., Han, H., Cheng, X., Wang, J., Feng, Y., Srinivas, S., Lu, G., Gao, G.F., 2014. Gluconate 5-dehydrogenase (Ga5DH) participates in *Streptococcus suis* cell division. Protein Cell 5, 761–769. https://doi.org/10.1007/s13238-014-0074-8.

Skagia, A., Zografou, C., Venieraki, A., Fasseas, C., Katinakis, P., Dimou, M., 2017. Functional analysis of the cyclophilin PpiB role in bacterial cell division. Genes Cells 22. https://doi.org/10.1111/gtc.12514.

Steele, V.R., Bottomley, A.L., Jorge, G.L., Jagath, K., Foster, S.J., 2011. Multiple essential roles for EzrA in cell division of Staphylococcus aureus. Mol. Microbiol. 80, 542–555. https://doi.org/10.1111/gtc.12514.

Vishnyakov, I.E., Borchsenius, S.N., 2007. FtsZ and bacterial cell division. Cell tissue biol. 1, 206–214. https://doi.org/10.1134/s1990519x07030029.

Wang, Y., Zhang, W., Wu, Z., Zhu, X., Lu, C., 2011. Functional analysis of *luxS* in *Streptococcus suis* reveals a key role in biofilm formation and virulence. Vet. Microbiol. 152, 151–160. https://doi.org/10.1016/j.vetmic.2011.04.029.

Wang, Y., Wang, Y., Liu, B., Wang, S., Li, J., Gong, S., Sun, L., Yi, L., 2019. *Pdh* modulate virulence through reducing stress tolerance and biofilm formation of *Streptococcus suis* serotype 2. Virulence 10, 588–599. https://doi.org/10.1080/21505594.2019.1631661.

Weart, R.B., Lee, A.H., An-Chun, C., Haeusser, D.P., Hill, N.S., Petra Anne, L., 2007. A metabolic sensor governing cell size in bacteria. Cell 130, 335–347. https://doi.org/10.1016/j.cell.2007.05.043.

Xiuzhen, P., Junchao, G., Ming, L., Bo, W., Changjun, W., Jing, W., Youjun, F., Zhimin, Y., Feng, Z., Gong, C., 2009. The orphan response regulator CovR: a globally negative modulator of virulence in *Streptococcus suis* serotype 2. J. Bacteriol. 191, 2601. https://doi.org/10.1128/JB.01309-08.

Zeeman, A.M., Luttik, M.A., Thiele, C., van Dijken, J.P., Pronk, J.T., Steensma, H.Y., 1998. Inactivation of the Kluyveromyces lactis KlPDA1 gene leads to loss of pyruvate dehydrogenase activity, impairs growth on glucose and triggers aerobic alcoholic fermentation. Microbiology 144 (Pt 12), 3437–3446. https://doi.org/10.1099/00221287-144-12-3437.